Michalowski, R. L. (1989). *Géotechnique* 39, No. 1, 27–38

Three-dimensional analysis of locally loaded slopes

R. L. MICHALOWSKI*

A three-dimensional slope stability analysis for drained frictional-cohesive material based on the upper-bound technique of limit analysis is presented. A rigid-block toe or above-the-toe collapse mechanism is considered, with energy dissipation taking place along planar velocity discontinuities. The technique is appropriate for slope analysis when question arises as to the level of permissible loads on slopes where the load is confined to a limited area (local load). The results in terms of limit loads are compared with those available in the literature for a particular case of a frictionless material. It was found that, for a wide variety of parameters (especially for large safety margins), the present analysis yields lower values of limit loads. Since they are rigorous upper bounds to the true limit load, these results should be considered as closer to the actual limit load.

KEYWORDS: bearing capacity; limit state analysis; slopes; stability.

Une analyse à trois dimension de la stabilité d'une pente pour un matériaux drainé et basée sur la technique de la limite supérieure est présentée. Un mécanisme d'éffondrement du bloc au pied ou au dessus du pied est considéré avec une dissipation d'énergie le long de discontinuitées planaires de vitesse. L'analyse en trois dimension présentée dans cet article est une technique convenable pour l'analyse d'une pente lorsque le niveau de la surcharge possible sur une pente est considérée et lorsque la surcharge est confinée à une aire limitée (surcharge locale). Les résultats en terme de surcharge critique sont comparés avec les résultats disponibles publiés pour le cas particulier d'un matériaux sans friction. On a trouvé que pour des pentes avec des marges de securité, l'analyse donne des valeurs plus faibles des surcharges critiques et, puisqu'il s'agit d'une borne supérieure rigoureuse par rapport à la vraie surcharge, ces résultats doivent être considérés plus près de la vraie valeur.

NOTATION

a	distance from slope crest to beginning of loading
b	width of loading
c	cohesion of soil
d	length of failure mechanism
F_2	2-dimensional factor of safety
F_3	3-dimensional factor of safety
k	block number
h	slope height
l	length of load
n	total number of blocks
N_s	stability factor
q	average limit pressure
S	boundary
T_i	true limit stress vector
v	volume
V_i	velocity vector
V_k	velocity of block k
$[V]_k$	velocity jump between blocks
Vol_k	volume of block k
X_i	body force vector
α_k, η_k, ξ	geometrical parameters of slope failure mechanism
β	slope angle
γ	specific weight
$\dot{\varepsilon}_{ij}$	strain tensor
μ	load multiplier
σ_{ij}	stress tensor
ϕ	internal friction angle

Discussion on this Paper closes on 3 July 1989. For further details see p. ii.

* University of Minnesota.

INTRODUCTION

Many practical geotechnical problems involving evaluation of admissible loads require three-dimensional (3-D) analyses, yet in most cases a traditional plane-strain analysis is used. This pertains to such important engineering issues as bearing capacity of rectangular footings or slope stability under local loads. This Paper is concerned with the problem of stability of slopes.

At least four different formulations of the slope stability problem can be distinguished: in terms of the factor of safety, the limit load of the slope, the critical height (maximum height) of the slope,

and the optimal shape of the slope. The analysis presented in this Paper concerns only the first two cases and is based on the upper-bound approach of limit plasticity.

Most of the methods for estimating the factor of safety are based on the equilibrium of (usually vertical) slices (2-D analysis). Variations of the slice method were presented by Fellenius (1927), Bishop (1955), Janbu (1957), Morgenstern & Price (1965) and Spencer (1967). The shape of the slip surface (or its location) corresponding to the minimum value of the safety factor is sought using various searching techniques. The slice approach seems to imply a mechanism of slope failure which involves sliding along the assumed slip surface. No restrictions, such as kinematical admissibility, are placed on that mechanism. The approach is purely static, based on a global equilibrium of slices, and the flow rule for the material (constitutive relation) is not even mentioned. If a simple perfectly plastic model of the soil is postulated with the Mohr-Coulomb yield condition and the associated flow rule, then collapse mechanisms implied by the slice methods are usually kinematically inadmissible (e.g. a rigid rotation mechanism for an assumed cylindrical slip surface in frictional materials). Statical admissibility of the stress field is also not satisfied, as some arbitrary assumptions are made to remove statical indeterminacy and as only a global equilibrium of slices is required. In some methods even this requirement is relaxed, as the number of global equilibrium equations that are satisfied for a single slice is reduced from three to two or one.

Validation of methods based on such approximate concepts, in terms of accuracy, without reference to more rigorous analyses, does not seem possible. None of these methods can be considered exact, and thus there is no solution available against which the results could be checked. It is only a hypothesis (used by a number of authors) that the more equilibrium equations there are satisfied (generally three for every slice under plane-strain conditions), the more accurate the method. In the case where both kinematical and statical admissibility is violated, any such hypothesis seems to be risky. It is only fair to conclude that since the concept of slice limit equilibrium is of an approximate nature, none of the methods utilizing this concept is accurate.

A rigorous 2-D analysis of slopes, based on the upper-bound theorem of limit analysis, was presented by Chen, Giger & Fang (1969) (see also Chen & Giger, 1971; Chen, 1975). Although the problem was formulated in terms of a critical height, the stability factors (as defined by Chen *et al.*) can be transformed into the factors of safety (for slopes with no external load and material with non-zero cohesion).

Two-dimensional analyses, although helpful for designing most slopes and embankments, are not applicable to slopes with distinct local loads. However, in practice, because no established 3-D method exists, slopes loaded locally are analysed by means of 2-D methods, assuming loads of an infinite extent. This may lead to a very conservative design.

A few approaches to 3-D analysis of slope stability have been proposed in the past decade or so. The method proposed by Hovland (1977) and Chen & Chameau (1982) (see also Hungr, 1987) seems to be an explicit extension of the plane-strain slice method. To account for the spatial failure mechanism the slices were replaced by columns, and equilibrium of the columns was required. The 3-D column method inherits the approximate nature of slice analysis, and questions as to the relevance of assumptions and accuracy of results cannot be answered easily.

Another approach to 3-D analysis was proposed by Baligh & Azzouz (1975) (see also Baligh, Azzouz & Ladd, 1977; Bliz, Brödel & Reinhardt, 1981; Azzouz & Baligh, 1983). These authors used a slice technique in order to evaluate limit loads or safety factors of slopes. In the particular case analysed by Azzouz & Baligh (1983) (frictionless material and cylindrical slip surface with conical caps), the slice method solution may provide the same results as the upper-bound solution for the rigid rotation mechanism. An extensive analysis of rotational 3-D mechanisms with a cylindrical centre part was presented recently by Gens, Hutchinson & Cavounidis (1988). However, the results obtained by Azzouz & Baligh and those by Gens *et al.* cannot be generalized to frictional soils.

A variational analysis was applied to the 3-D slope stability problem by Leshchinsky, Baker & Silver (1985). Their approach was based on a limit-equilibrium method, and the solution provides two potential failure surfaces, one of which is truly a 3-D surface. Not surprisingly, the solution corresponding to the 3-D mechanism yields factors of safety higher than those for 2-D failure, and the results following from the 2-D failure mechanism are identical to those shown by Chen (1975) (the results were presented by Leshchinsky *et al.* (1985) in terms of a stability number which is the inverse of Chen's stability factor).

The method for the analysis of slope stability presented in this Paper is based on the kinematical approach of limit analysis. This technique was applied by Drescher (1983) to 3-D stability analysis of vertical cuts. This analysis was related to forming empty channels in storage bins for granular materials. The present analysis can be regarded as an extension of Drescher's analysis to more complex failure mechanisms.

The analysis presented here is mathematically rigorous, although it yields only the upper estimation of the limit load (or the factor of safety). It is believed, however, that the 3-D analysis presented is more appropriate as an engineering tool than other available methods, especially if it shows that the limit loads or the factors of safety obtained are lower than those from other methods.

THEOREMS OF LIMIT ANALYSIS

The theorems of limit analysis constitute a useful tool for analysing problems in which a limit load is to be found. These theorems are explicit extensions of the *principle of maximum work* derived by Hill (1948), and were given in the form of theorems by Drucker, Greenberg & Prager (1952). The following assumptions are made: (a) the material is perfectly plastic at the limit state; (b) the limit state is described by a yield function $f(\sigma_{ij}) = 0$, convex in the stress space σ_{ij}; and (c) the material obeys the potential flow rule associated with the yield condition

$$\dot{\varepsilon}_{ij} = \dot{\lambda} \frac{\partial f(\sigma_{ij})}{\partial \sigma_{ij}}, \quad \dot{\lambda} \geqslant 0 \tag{1}$$

where $\dot{\varepsilon}_{ij}$ is the strain rate tensor, σ_{ij} is the stress tensor and $\dot{\lambda}$ is a non-negative scalar function.

The application of the first, lower-bound theorem, is based on the construction of statically admissible stress fields. Such stress fields must satisfy statical boundary conditions and equations of statical equilibrium at every point of the material, and must not violate the yield function of the material, i.e. the stress state can be either at its limit (limit state) or below. The first theorem states that a statically admissible stress field supplies a load which is not higher than the true limit load.

Applications of the second theorem are based on the construction of kinematically admissible velocity fields. Such fields have to comply with the kinematical boundary conditions and compatibility conditions following from flow rule (1). The second, upper-bound theorem, can be expressed as: if a kinematically admissible velocity field is found, then the load obtained from such field, through the balance of external forces' work and internal dissipation, is not lower than the true limit load.

These theorems are true when the load to be found is active, i.e. when the direction of load action is the same as the displacement direction of the loaded boundary. If the reactions are to be found, then the first (statical) theorem yields the upper bound, and the second (kinematical) the lower bound to the true value of the reaction. In order for the solutions to be valid, the deformations before the limit state need to be negligible. This requirement is necessary for the principle of virtual work to be applicable.

The theorems of limit analysis do not provide the exact value of the true limit load, but two bounding values. It would seem natural, then, to use both theorems in order to estimate the range in which the true limit load is contained and to try to perform the analysis in such a way as to minimize this range, so that a precise judgement as to the actual limit load (or factor of safety) can be made. Unfortunately, this is not always possible.

Kinematical velocity fields (mechanisms) used to obtain upper bounds usually have a distinct physical interpretation, associated with true collapse mechanisms (known from experiments or practical experience). Stress fields used in the lower-bound approach, however, are constructed without a clear relation to real stress fields, other than the stress boundary conditions. Moreover, in geotechnics, where the formulation of problems often involves a semi-infinite half-space, the extension of the stress field into the half-space is either cumbersome or seems to be impossible. There are only a few non-trivial solutions in geotechnical engineering for which the extension into the far field has been found. In most cases, even though the stress field may be found using the rigorous method of characteristics (plane-strain problems), the extension of the solution beyond the domain determined by the hyperbolicity of the statical equations meets certain difficulties. Because of the problems with constructing admissible stress fields, only the upper-bound (kinematical) approach will be used in this Paper.

Upper-bound solutions based on kinematically admissible rigid-block velocity fields (associated with the linear Mohr-Coulomb yield condition) satisfy global force equilibrium equations (Appendix 1). Hence, in some cases, the limit-equilibrium method may yield the same results as the rigorous upper-bound approach. By no means, however, can the two methods be regarded as equivalent. This is discussed in more detail in Appendix 1.

FORMULATION OF THE PROBLEM

This Paper presents a consistent analysis, based on the kinematical theorem of limit plasticity, which can be used to obtain both the limit load of slopes (load necessary to produce failure) and the factor of safety, and which can be applicable in both 2-D and 3-D cases of slope failures.

The soil is considered to be isotropic and perfectly plastic, and to obey both the Mohr-Coulomb yield condition and the associated flow rule. The unknown load is assumed to be vertical.

Deformations of the slope before the limit state are considered to be negligible.

Almost ideal applications of the upper-bound theorem are those in the plastic forming of metals, where the movement of a tool-piece is well-defined (boundary condition) and the kinematical approach yields the upper, and thus 'safe', estimation of forces necessary for the deformation process to take place. In geotechnics, besides the fact that the upper bound is an 'unsafe' estimation, the kinematical boundary condition is usually not well-defined. In the problem of bearing capacity of footings, for example, it only can be assumed that the loaded boundary moves in a rigid-motion manner, but the relationship between the translation and the rotation of the footing cannot be given *a priori*. The problem of a slope limit load does not have a well-defined kinematical condition either. In fact, in this case, even the assumption of a rigid-motion boundary may not be true. Nevertheless, solutions presented in this Paper are obtained solely for the boundary condition defined as a rigid translation. This does not contradict the rigour of the kinematical approach, and the results will still be upper bounds to the true limit load.

The slope stability problem is traditionally formulated in terms of a factor of safety. Such formulation seems to have an advantage over that of the limit load. The loading of slopes consists, for the most part, of the weight of the material itself. It would be difficult, however, to make a distinction between the part of the material which loads the slope and that which resists the collapse. The factor of safety makes this distinction unnecessary.

A generally accepted definition of the safety factor is that given by Bishop (1955): the ratio of the available shear strength of the soil to that required to maintain equilibrium. If it is assumed that the material effort is equally attributed to cohesion and internal friction, a useful form of the safety factor is obtained

$$F = c/c_m = \tan \phi/\tan \phi_m \qquad (2)$$

where c and ϕ are the actual cohesion and internal friction angle of the material, and c_m and ϕ_m are the parameters required to maintain the limit equilibrium. This definition is used throughout this Paper. In order to obtain a unique solution it is necessary to assume that the material effort is the same along all of the shear surfaces (i.e. there is one factor of safety describing the strength mobilization along all failure surfaces). The factor of safety is a function of the geometrical parameters of the collapse mechanism (the geometry of the slope and material parameters being constant for a given slope), and it is useful information only if it corresponds to its minimum value.

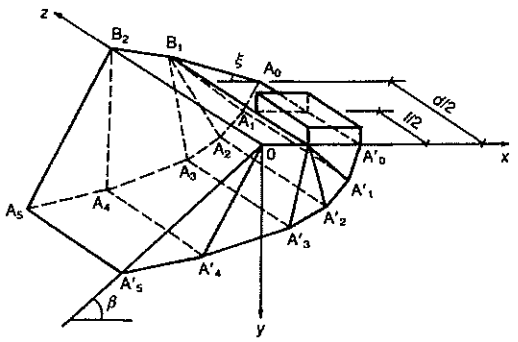

Fig. 1. The collapse mechanism (x0y is the plane of symmetry)

ASSUMED COLLAPSE MECHANISM OF A LOCALLY LOADED SLOPE AND THE PROBLEM SOLUTION

The mechanism of failure used in the analysis is shown in Fig. 1. It consists of rigid-motion blocks separated by planar velocity discontinuity surfaces. Although only five blocks are shown in Fig. 1, the number of blocks can be increased without any extra analytical effort (up to 50 blocks were considered in the calculations). An external load is located on a rectangular area, as shown in the figure. All blocks have a prismatic shape, with triangular or quadrangular bases. In the particular case where the loading extends to the crest of the slope, all blocks have triangular bases.

To calculate the work rate of the external forces and the internal work dissipation rate, the velocities of all blocks have to be known. However, the velocity on the loaded boundary is not well-defined. Collapse of a slope will probably involve a combination of translation and rotation. It is assumed in this analysis, however, that the loaded area does not rotate. If rotation were assumed as a boundary condition, then the limit load could be estimated only in terms of a moment, and an additional assumption would be required as to the distribution of the load in order to determine the limit force. Rotation of the loaded boundary (e.g. around axis $A_0 A_0'$ in Fig. 1) would produce continual deformation in the soil mass. Only rigid block mechanisms are considered in this Paper.

Using the trigonometric relationships shown in Fig. 2, the velocities V_k of blocks ($k = 1, 2, 3 \ldots n$, n being the number of blocks) and the velocity jumps between the blocks $[V]_k$ can be derived. Note that in kinematically admissible mechanisms, velocity increment vectors across velocity discontinuity surfaces have to be inclined to those surfaces at the internal friction angle ϕ (associative flow rule). Angles α_k and η_k (Fig. 2) and ξ (Fig. 1) are here assumed to be known. The

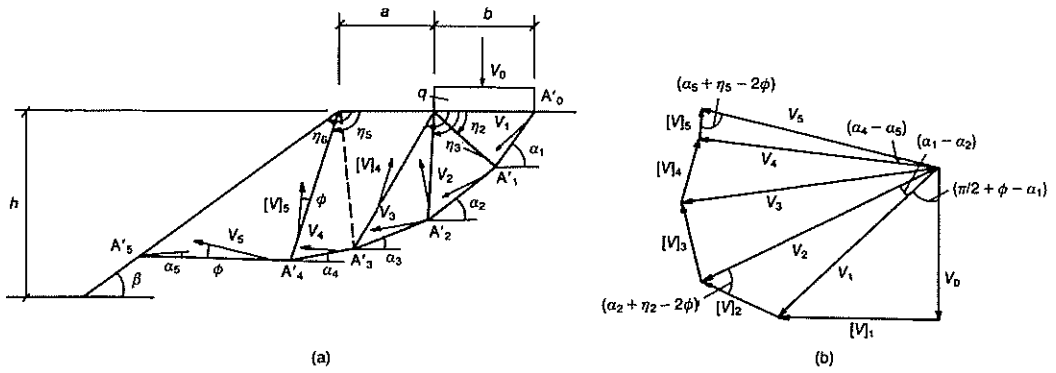

Fig. 2. (a) Cross-section of a collapse mechanism; (b) hodograph

velocity magnitude of the first block is $V_1 = V_0/\sin(\alpha_1 - \phi)$. For all other blocks, two cases have to be considered. For the first case, when $\alpha_k \leqslant \alpha_{k-1}$, $k = 2, 3, 4 \ldots n$

$$V_k = V_{k-1} \frac{\sin(\eta_k + \alpha_{k-1} - 2\phi)}{\sin(\eta_k + \alpha_k - 2\phi)} \tag{3}$$

$$[V]_k = V_{k-1} \frac{\sin(\alpha_{k-1} - \alpha_k)}{\sin(\eta_k + \alpha_k - 2\phi)} \tag{4}$$

and the condition

$$\eta_k + \alpha_k - 2\phi > 0 \tag{5}$$

has to be satisfied in order for the mechanism to be kinematically admissible. For the second, when $\alpha_k > \alpha_{k-1}$, $k = 2, 3, 4 \ldots n$

$$V_k = V_{k-1} \frac{\sin(\eta_k + \alpha_{k-1})}{\sin(\eta_k + \alpha_k)} \tag{6}$$

$$[V]_k = V_{k-1} \frac{\sin(\alpha_k - \alpha_{k-1})}{\sin(\eta_k + \alpha_k)} \tag{7}$$

and the necessary condition is

$$\pi - \alpha_k - \eta_k > 0 \tag{8}$$

With the geometry of the mechanism known in cross-section $x0y$ (Fig. 2(a)), and the velocities now determined, the planes limiting the mechanism on its 'ends' can be found. The 'end planes' must be inclined to the velocity vectors at angle ϕ. Analytical geometry relations were used in order to find the 'end surfaces', as well as the surface areas of blocks and their volumes (Appendix 2).

Having the velocities of all blocks, as well as their volumes and surface areas, the upper bound to the limit load can be found. The upper-bound theorem can be written in the form

$$\int_S V_i T_i \, dS \leqslant \int_v \sigma_{ij}^* \dot{\varepsilon}_{ij}^* \, dv - \int_v X_i V_i^* \, dv \tag{9}$$

where T_i is the unknown true limit stress vector on boundary S where velocity vector V_i is prescribed (indices i and j denote cartesian coordinates; $i, j = 1, 2, 3$), and v is the volume. Note that, in general (when V_i is not constant on S), inequality (9) allows one to determine the upper bound to the work (rate) of the unknown (limit) force, rather than the upper bound to the limit force itself. The first term on the right-hand side of inequality (9) denotes the rate of work dissipation within the material, where $\dot{\varepsilon}_{ij}^*$ is the assumed field of admissible deformation (rate) and σ_{ij}^* is the stress field related to $\dot{\varepsilon}_{ij}^*$ through the flow rule (equation (1)). The last term in inequality (9) denotes the work rate of body forces, X_i being the body force vector. Introducing a load multiplier μ, such that $\mu \geqslant 1$, and assuming that boundary S undergoes a rigid translation with given velocity V_i^0 ($V_i = V_i^0$ on S), inequality (9) can can be written as

$$\mu V_i^0 \int_S T_i \, dS = \int_v \sigma_{ij}^* \dot{\varepsilon}_{ij}^* \, dv - \int_v X_i V_i^* \, dv \tag{10}$$

Work dissipation per unit area of a discontinuity surface within the cohesive-frictional material can be expressed as

$$\dot{D} = [V]c \cos\phi \tag{11}$$

where $[V_c]$ is the magnitude of the velocity jump and c is the cohesion. For the particular rigid-block mechanism considered, where the only energy dissipation takes place along velocity dis-

continuities, equation (10) can be written as

$$\mu T V_0 = c \cos \phi \sum_{k=1}^{n} S_k' V_k + c \cos \phi \sum_{k=1}^{n} S_k''[V]_k - \gamma \sum_{k=1}^{n} Vol_k V_k \sin(\alpha_k - \phi) \quad (12)$$

where μT is the upper bound to the true (vertical) limit load T (μ being a dimensionless coefficient, $\mu \geqslant 1$). V_0 is the vertical velocity component of the loaded boundary, γ is the specific weight, and n is the number of blocks. Vol_k is the volume of block k, and S_k' and S_k'' are the areas along which jumps V_k and $[V]_k$ occur, respectively.

The set of angles α_k, η_k ($k = 1, 2, 3 \ldots n$) and angle ξ so far have been assumed to be known. Any set of these angles that would produce an admissible mechanism of a slope failure would provide an upper bound to the true limit load. A numerical technique was used in the computations in order to find the set corresponding to the least upper-limit load. This technique was based on a simple algorithm where, in one computational loop, angles α_k, η_k and ξ were changed twice by step $\Delta\alpha$ ($-\Delta\alpha$ and $+\Delta\alpha$), and the value of the limit load was calculated after each change. If the variation caused the limit load (or factor of safety) to decrease, then the value of the respective angle was changed accordingly (by $\pm\Delta\alpha$). Step $\Delta\alpha$ was decreased in computations from 5° to 0·1°. The calculations were continued until two subsequent loops yielded the same limit load (with $\Delta\alpha = 0{\cdot}1°$). The minimum limit force always corresponds to $d = l$ (Fig. 1).

If the slope stability problem is formulated in terms of the factor of safety, the algorithm for computing velocities, areas and volumes of blocks and the searching procedure are virtually the same. Now, however, force T in equation (12) is the known boundary condition. The factor of safety is then found by the iteration technique, in which the values of cohesion c and $\tan\phi$ are dropped at the same rate until equation (12) is satisfied. The last ratio in the iteration procedure is then equal to the factor of safety defined by equation (2). Coefficient μ is not known, and the slope loading is substituted for μT in equation (12). This procedure yields the upper estimation to the true factor of safety defined by equation (2).

COMPUTATIONAL RESULTS

The mechanisms of deformation used here to predict limit loads consist of rigid motion blocks (Fig. 1), and there is no mechanical limitation as to the number of blocks. As expected, it was found that the limit load obtained from the proposed analysis approaches an asymptotic value when the number of blocks in the mechanism considered is increased.

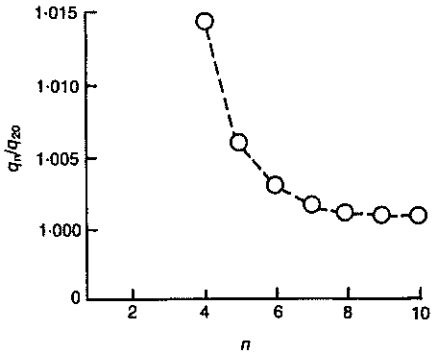

Fig. 3. Typical decrease of the calculated limit load with increasing number of blocks n (q_{20} is the load calculated for a 20-block mechanism). The calculations have been made for data from Fig. 6(a) ($\beta = 15°$, $a/h = 0{\cdot}1$)

All results presented in this Paper are from calculations with six-block mechanisms. It was found that an increase of the number of blocks beyond six (up to 50) produced a drop in the limit load of less than 1%. A typical decrease of the limit load with an increasing number of blocks is shown in Fig. 3. The computer program was written in such a way as to allow a minimum of four blocks.

All values of limit loads and factors of safety (or respective ratios) presented in this Paper correspond to geometries of failure mechanisms which yield the lowest values of the loads or factors. Three-dimensional analysis in terms of the factor of safety presented in this paper makes sense only for locally loaded slopes. If no local loading is declared, angle ξ (see Fig. 1) tends to 90°, and the minimum value of the safety factor approaches that in 2-D analysis. This is to be expected, since, for mechanisms where all velocity vectors are parallel to one plane (perpendicular to the crest), a 2-D failure mechanism yields the minimum of the safety factor (Cavounidis, 1987 (Cavounidis used a different definition of the factor of safety)).

Figure 4 shows the factor of safety F_3 obtained from the 3-D analysis of a locally loaded slope as a function of ratio d/l (d being the length of the failure mechanism, and l the length of the load). It is seen that when d increases, but the local load is kept fixed, the 3-D factor of safety approaches the 2-D factor obtained from an analysis with no load condition. This is to be expected; when d approaches infinity, the influence of a local load vanishes, and the influence of the 'end effects' on the 3-D safety factor becomes negligible. However, depending on the level of the local load,

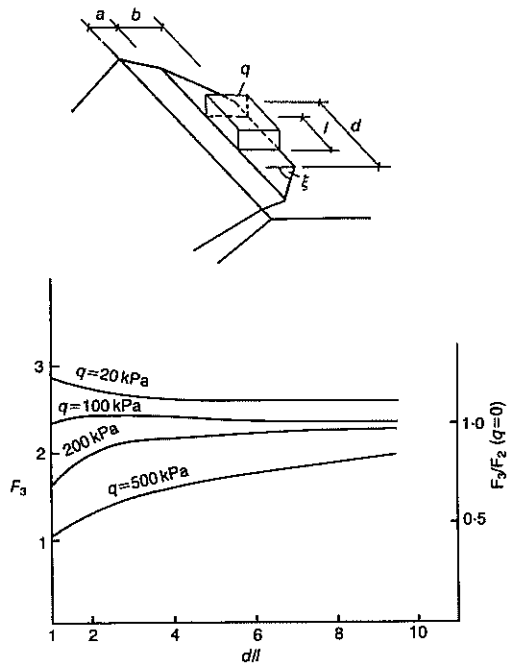

Fig. 4. Safety factors from 3-D analysis presented in this Paper for a locally loaded slope, as functions of the length of the collapse mechanism for different magnitudes of the load; $\phi = 20°$, $c = 20$ kPa, $\gamma = 20$ kN/m^3, $\beta = 30°$, $h = 10$ m, $a = 1$ m, $b = 2$ m, $l = 3$ m

a 3-D analysis may provide higher or lower values of the safety factor than a 2-D analysis with no external load.

It follows from Fig. 4 that the minimum of the safety factor is always obtained either from plane-strain analysis or from 3-D computations with $d = l$. Thus, in hypothetical experiments with locally loaded homogeneous slopes (of infinite length), a 3-D collapse mechanism (with $d = l$) will always occur, since before loading, the experimental slopes have to be stable ($F_2 > 1$). A plane-strain collapse of a locally loaded slope could theoretically be induced in a centrifuge, where the load would be exerted by an elastic element (e.g. a spring) with a small mass (so that the increase of the load due to the increase of acceleration could be neglected).

If a traditional plane-strain analysis is applied to slopes with confined loads (i.e. if the local load is taken as a strip load in the computations), then the resulting factor of safety is lower than that obtained from 3-D analysis. These factors are usually utilized in design procedures; however, they should be considered very conservative. Fig. 4 suggests that small loads can be neglected in the analysis (e.g. $q = 20$ kPa for the particular case shown in Fig. 4), and the 2-D factor of safety (for the $q = 0$ condition) seems to be an appropriate design parameter in such cases. For higher loads, 3-D analysis yields safety factors lower than those from 2-D analysis (and $q = 0$), but not as low as the 'traditional' 2-D analysis with loads extended to strip loads. For those larger loads, the 3-D analysis presented here can be regarded as a less conservative design (in fact, this approach is not conservative at all, as it is based on the upper-bound theorem of limit analysis).

Figures 5 and 6 show the limit pressure ratio q/c (obtained using the proposed analysis) for cohesive slopes with square loads, and those for frictionless soils obtained by Azzouz & Baligh (1983). The comparison is shown for slopes with a margin of safety $\Delta(\gamma h/c)$ equal to 3·0 (Fig. 5) and equal to 1·0 (Fig. 6). The margin of safety used here was defined by Azzouz & Baligh as the difference between the stability factor $(\gamma h/c)_{cr}$ and the factor $\gamma h/c$ for the actual slope (this margin of

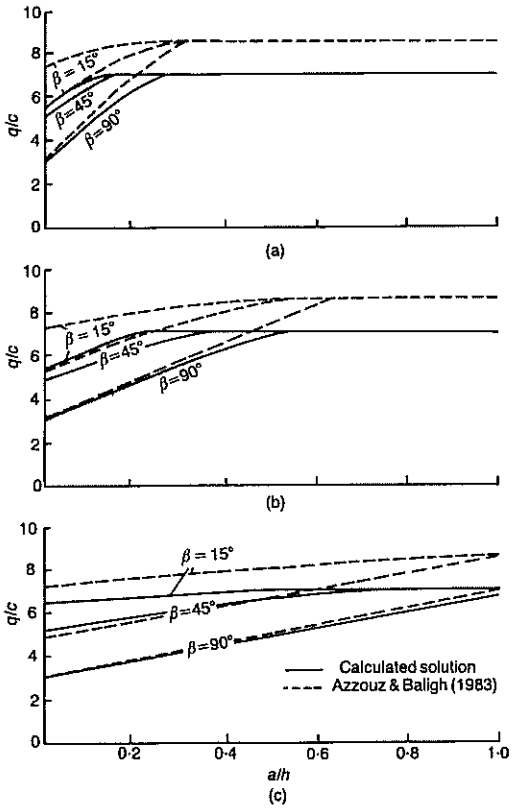

Fig. 5. Limit pressure ratios for square loaded ($l/b = 1·0$) frictionless slopes with margin of safety $\Delta(\gamma h/c) = 3·0$, compared with results from Azzouz & Baligh (1983): (a) $b/h = 0·25$; (b) $b/h = 0·50$; (c) $b/h = 1·00$

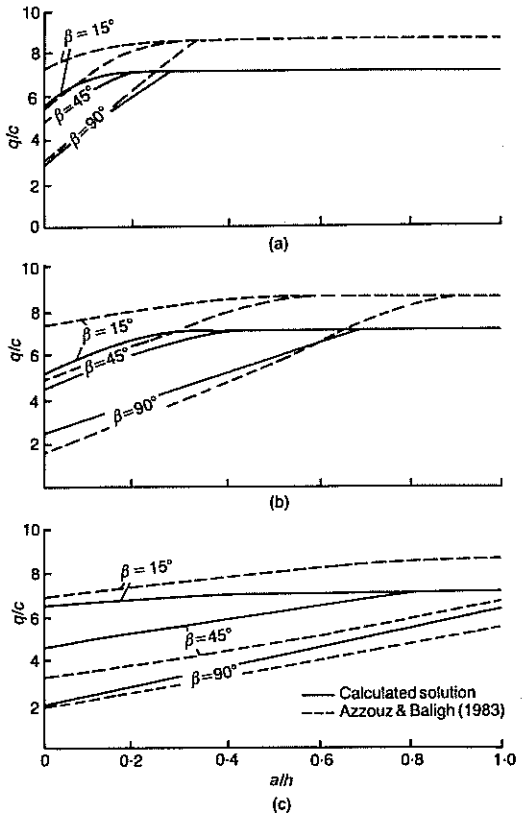

Fig. 6. Limit pressure ratios for square loaded ($l/b = 1{\cdot}0$) frictionless slopes with a small margin of safety ($\Delta(\gamma h/c) = 1{\cdot}0$): (a) $b/h = 0{\cdot}25$; (b) $b/h = 0{\cdot}50$; (c) $b/h = 1{\cdot}00$

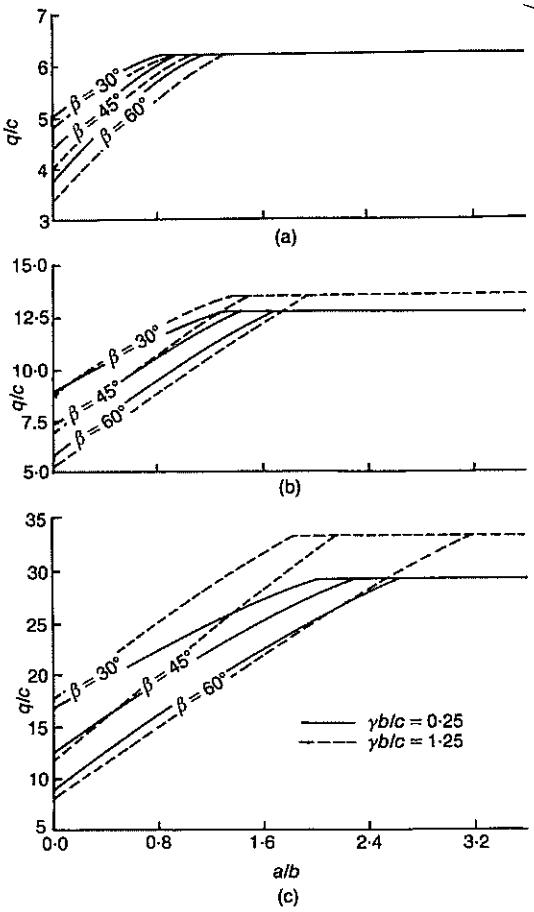

Fig. 8. Dimensionless limit pressures of a slope (frictional/cohesive soil): $l/b = 2{\cdot}0$; (a) $\phi = 0°$; (b) $\phi = 10°$; (c) $\phi = 20°$

safety depends on the method used for estimating $(\gamma h/c)_{cr}$). For the purpose of making the comparison possible, the following stability factors were adopted: for a vertical cut, $\beta = 90°$, $N_s = (\gamma h/c)_{cr} = 3{\cdot}83$; for $\beta = 45°$, $N_s = 5{\cdot}86$; and for $\beta = 15°$, $N_s = 7{\cdot}35$ (see Chen, 1975). It seems that Azzouz & Baligh used the same values.

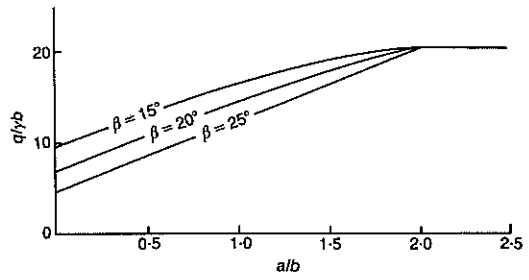

Fig. 7. Dimensionless limit pressures as functions of geometrical parameters of a slope (cohesionless soil); $\phi = 30°$, $c = 0$, $l/b = 2{\cdot}0$

The analysis presented here yields the upper bound to the true limit load, yet, for a wide range of parameters, the results obtained are lower than those found by Azzouz & Baligh (1983). Only if the margin of safety is small (e.g. 1·0) and the length of slope ($h/\sin\beta$) is less than about twice the width of the loaded area does Azzouz & Baligh's analysis yield lower values of the limit load (e.g. Fig. 6(c)). Including base (below-the-toe) failures in the analysis presented here might result in reducing the estimated loads for these specific examples.

It needs to be emphasized that the present objective was to include both cohesive and frictional shear strength of soil in the 3-D limit analysis of slopes. Comparisons of the results

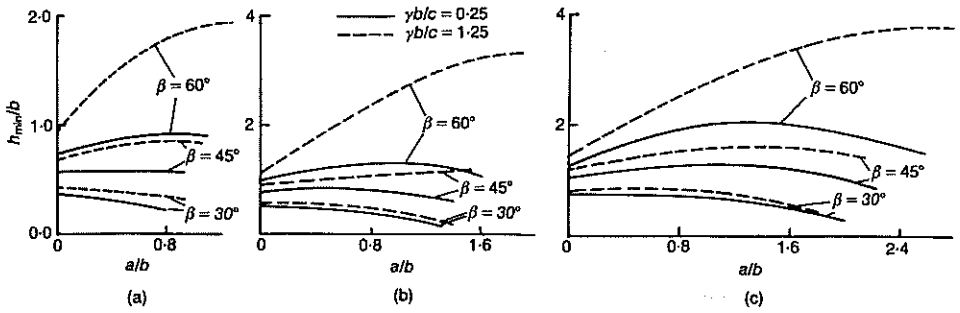

Fig. 9. Minimum height of slopes for which diagrams in Fig. 8 correspond to the most critical condition (Fig. 8 should not be used for slopes with smaller heights); $l/b = 2·0$: (a) $\phi = 0°$; (b) $\phi = 10°$; (c) $\phi = 20°$

with those for frictionless soil were made only because, so far, no (rigorous) 3-D results for frictional soils exist. These comparisons were made in order to verify the validity of the proposed approach.

A sample of the results from the analysis proposed in this paper, for frictional soils, is shown in Figs 7 and 8. Fig. 7 represents the dimensionless limit pressure on a cohesionless slope as a function of the distance of the load from the crest of the slope. Similar diagrams for frictional-cohesive slopes are shown in Fig. 8. The examples are independent of the height of the slope, since only above-the-toe failures are considered. In all examples the slopes were high enough to allow above-the-toe failures, but not so high as to exceed the stability factor $N_s = (\gamma h/c)_{cr}$. The minimum slope heights for which the results presented in Fig. 8 should be considered applicable is shown in Fig. 9, and the maximum slope heights in Fig. 10.

Figures 7 and 8 can easily be converted to resemble Figs 5 and 6 by first assuming the ratio $K = b/h$, and then replacing b in parameters $\gamma b/c$ and a/b with Kh.

The effect of the 3-D collapse mechanism in the stability analysis of locally loaded slopes is shown in Fig. 11, where a dimensionless limit pressure is shown as a function of the length-to-width ratio (l/b) of the local load. As expected, the limit pressure drops as ratio l/b increases, and it approaches the value from plane strain analysis. All the curves in Fig. 10 are limited by the dotted line, which represents the limit pressure for 3-D foundation-type failure on the top of the slope.

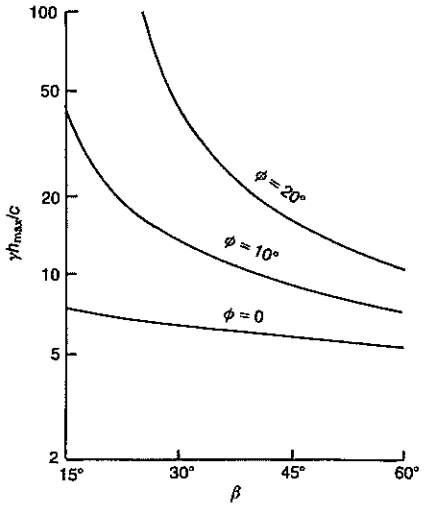

Fig. 10. Maximum height of slopes for which results in Fig. 8 are considered to be applicable (equal to critical height of plane slopes (Chen, 1975))

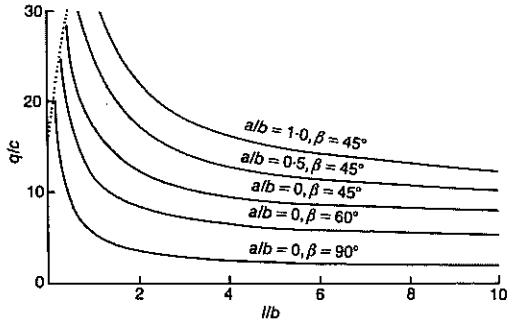

Fig. 11. Limit load on slopes as a function of the length-to-width ratio of the local load; $\phi = 20°$, $\gamma b/c = 1·25$

CONCLUSIONS

An analysis of locally loaded slopes, based on the upper-bound approach of limit plasticity, has

been described. The method allows for evaluation of the factor of safety or the limit load applied to a slope. Examples for homogeneous soils with drained strength described by the Mohr-Coulomb yield condition were given. Modifications of the assumed collapse mechanism could, however, accommodate some patterns of non-homogeneity (e.g. horizontal layers).

The method provides the solution for both cohesive and frictional soils. The proposed approach provides the upper bound to the true limit load (or the factor of safety), yet, for a wide range of parameters, yields lower loads than those available in the literature for frictionless soils.

The analysis presented here was related originally to stability of waste rock mine dumps (with relatively small grain dimensions) under loads from heavy dump trucks. Therefore, the analysis includes only local loss of stability (the above-the-toe collapse mechanism and the failure surface crossing through the contour of the load), as happens when a loaded truck reaches the area close to the crest of a dump slope.

The analysis given could be improved by including the below-the-toe mode of failure. The method as presented is valid in all cases of homogeneous locally loaded slopes, in that it always yields the upper estimation to the true limit load. Considering base (below-the-toe) failure mode, however, could result in a lower overestimation of limit loads for some slopes.

As expected, it was found that, for slopes with no external load, the mechanism of failure (which is being modified in the course of searching for the minimum value of the limit load or factor of safety) tends to a plane-strain case. Three-dimensional analysis becomes important only when the slope is locally loaded; it may also be important when the length of a slope is physically restrained or when local non-homogeneities in soil parameters occur.

The analysis is useful whenever the question arises as to the level of permissible loads on slopes, when the load is clearly confined to a limited area. It also can be helpful in estimating factors of safety of locally loaded slopes. For cases where no external load is present, or the load is very small, the mechanism which yields the minimum factor of safety tends to the plane-strain mechanism.

The analysis described is related to the classical approach to the slope stability problem. Including elastic properties of soil and its softening characteristic in the plastic range of deformation could result in predictions of 'progressive failure' of slopes where the peak strength is not reached simultaneously on all sliding (shear) surfaces. Such analysis could also predict the scale effect observed in practice in many engineering problems related to ultimate loads. It seems that continuation of the study should follow in this direction.

ACKNOWLEDGEMENTS

The Author benefited from discussions with Professor A. Drescher of the University of Minnesota, and would also like to express his gratitude to the US Bureau of Mines for sponsoring part of the research reported in this Paper.

APPENDIX 1

The equivalence of the *results* for limit load problems obtained using the upper-bound theorem of limit analysis and the limit-equilibrium method has been mentioned in the literature on a few occasions. In some cases the two methods may indeed yield the same results. However, as noticed by Collins (1974), Chen (1975), and others, the two *methods* are not equivalent.

The upper-bound technique of limit analysis can be regarded as a particular case of the energy balance approach, as it is based on the energy (rate) balance equation. In general, energy balance does not supply the upper bound to the true limit load. Both the limit equilibrium method and the energy balance approach require that a pattern of deformation (kinematical mechanism) is assumed. The major difference between the two techniques is in the extent of assumptions made as to the material's behaviour. The limit equilibrium method requires that only the yield condition be specified, while for the energy balance approach it is necessary to specify both the yield condition and the flow law. The limit equilibrium method will work only if the kinematical mechanism consists of rigid-motion blocks and is such that a force polygon can be uniquely constructed for each block (i.e. a set of global static equilibrium equations is determinable for each block).

The energy balance approach is not limited to rigid-block mechanisms. Energy dissipation within the mechanism cannot be calculated, however, without assuming a particular relationship between the strain-rate tensor and the stress tensor (flow rule). The energy balance solutions can be proven upper bounds to the true limit load only if: the yield condition specified for the material is convex in the stress space; the flow rule is associated with this condition (see equation (1)); and the failure mechanism for which the work (rate) balance is considered is kinematically admissible (i.e. satisfies kinematical boundary conditions and obeys the associative flow rule). Note that, unlike in the limit-equilibrium method, static equilibrium is not required in the energy balance approach.

In further considerations, the energy balance method is restricted here to the upper-bound approach. It is discussed in the following when upper-bound solutions satisfy global static equilibrium, and the limit loads from both limit-equilibrium and upper-bound techniques are the same.

Let block OAB in Fig. 12 be part of a kinematically admissible plane mechanism. Boundaries S_1, S_2 and S_3 are loaded with distributed loads T_i. Block OAB moves

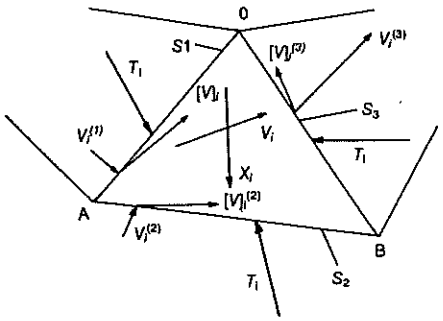

Fig. 12. Rigid block with boundaries determined by surfaces S_1, S_2 and S_3

with velocity V_i, and adjacent blocks move with velocities $V_i^{(1)}$, $V_i^{(2)}$ and $V_i^{(3)}$ respectively. Thus, velocity jump vectors on S_1, S_2 and S_3 are

$$\begin{aligned}[V]_i^{(1)} &= V_i - V_i^{(1)} \\ [V]_i^{(2)} &= V_i - V_i^{(2)} \\ [V]_i^{(3)} &= -V_i + V_i^{(3)}\end{aligned} \tag{13}$$

The balance of the internal work dissipation and of external forces work can be written for a single block as

$$\begin{aligned}-\int_{S_1} T_i[V]_i^{(1)}\,dS_1 - \int_{S_2} T_i[V]_i^{(2)}\,dS_2 \\ + \int_{S_3} T_i[V]_i^{(3)}\,dS_3 = \int_{S_1} T_i V_i^{(1)}\,dS_1 \\ + \int_{S_2} T_i V_i^{(2)}\,dS_2 + \int_{S_3} T_i V_i^{(3)}\,dS_3 + \int_v X_i V_i\,dv\end{aligned} \tag{14}$$

After using the compatibility conditions (equation (13)), all terms with velocities other than V_i vanish, and equation (14) can be written as

$$V_i\left\{\int_{S_1} T_i\,dS_1 + \int_{S_2} T_i\,dS_2 + \int_{S_3} T_i\,dS_3 + \int_v X_i\,dv\right\} = 0 \tag{15}$$

The scalar product in equation (15) is equal to zero when either block velocity V_i is orthogonal to the total force vector (the sum in curly brackets) or the total force vector is equal to zero

$$\int_{S_1} T_i\,dS_1 + \int_{S_2} T_i\,dS_2 + \int_{S_3} T_i\,dS_3 + \int_v X_i\,dv = 0 \tag{16}$$

Note that equation (16) is nothing else but the set of global force equilibrium equations which is used in the limit equilibrium method. A similar derivation can be pursued for a system of blocks. Equation (15) written for a multi-block system has the form of a sum of expressions similar to that on the left side of equation (15), one expression for each block.

If the entire mechanism consists of only one block, then the force acting on one side of the block, e.g. S_1, can be considered as limit load $\int P_i\,dS_1$ and the force acting on S_3 as given boundary condition $\int Q_i\,dS_3$. Equation (15) can be written now as

$$V_i\left\{\int_{S_1} P_i\,dS_1 + \int_{S_2} T_i\,dS_2 + \int_{S_3} Q_i\,dS_3 + \int_v X_i\,dv\right\} = 0 \tag{17}$$

Assume that block OAB (Fig. 12) slides over material at rest ($V_i^{(2)} = 0$) and that the material obeys the linear Mohr-Coulomb yield condition. Energy dissipation in the upper-bound approach is calculated assuming that the stress vectors along gliding surfaces (or the stress state within continually deforming regions) satisfy the yield condition. However, for the Mohr-Coulomb yield condition these stresses do not need to be specified, as the dissipation along discontinuities is independent of the stress components (see equation (11)). Static equilibrium will be satisfied by upper-bound solutions if there exists a vector $\int T_i\,dS_2$ satisfying the yield condition and assuring that the sum in braces in equation (17) is zero.

For a specified vector $\int T_i\,dS_2$, the sum in braces in equation (17) gives a certain vector $\Delta\int T_i\,dS$ (this vector is either zero or is orthogonal to velocity vector V_i). Therefore, for the specified vector $\int T_i\,dS_2 - \Delta\int T_i\,dS$ on S_2, the sum in curly brackets is zero. The upper bound solution will then satisfy global static equilibrium if vector $\int T_i\,dS_2 - \Delta\int T_i\,dS$ satisfies the yield condition. The last requirement is true for the Mohr-Coulomb yield condition, associated flow rule, and for a block sliding over material at rest ($V_i^{(2)} = 0$, Fig. 12). Hence, in this particular case, the upper-bound approach and limit-equilibrium method, based on identical failure mechanisms, supply identical limit loads. The same argument can be made for a multi-block system sliding over material at rest.

Static equilibrium of upper bound solutions is not, in general, satisfied when a non-linear yield condition is considered (in such case, the stress vector on boundary S_2 has to be specified before calculation of the energy dissipation rate). Also, static equilibrium cannot be proven for energy balance solutions where the non-associative flow rule for the material is assumed.

The kinematical approach of limit analysis does not lose its clear scheme if 3-D mechanisms are considered. As long as an admissible hodograph for the spatial mechanism is found, one component (or magnitude) of the limit force (upper bound) can be found. This is not the case with the limit-equilibrium method. The number of block interfaces for blocks in 3-D mechanisms is generally higher than that in 2-D mechanisms, and the set of global static equilibrium equations may not be determinable. For example, for the slope collapse mechanism considered in this Paper there are still only two non-trivial static equilibrium equations (symmetrical mechanism), but the number of unknowns for each block increases to four. Hence, no unique solution can be obtained using the limit-equilibrium method.

In conclusion, the upper-bound approach of limit analysis should be considered a more rigorous and more general approach to limit load problems than that using limit-equilibrium equations. Although in some particular cases the two methods may yield the same results, by no means should they be regarded as equivalent.

APPENDIX 2

The following algorithm was used to determine the end surfaces for the 3-D collapse mechanism shown in Fig. 1.

As the location of point A_0 is known (determined by the location of the load or otherwise), the co-ordinates of point B_1 can be found (angle ξ assumed). With co-ordinates of points A_0 and B_1 known, the unknown co-ordinate z of point A_1 can be determined (x and y for point A_1 are known, as α_1 and η_2 are assumed *a priori*, Fig. 2(a)). The direction of vector V_1 was analytically described as

$$\frac{x - x_0}{a} = \frac{y - y_0}{b} = \frac{z - z_0}{c} \tag{18}$$

(x_0, y_0, z_0 being co-ordinates of a point on this direction) and plane $A_0B_1A_1$ was analytically defined as

$$Ax + By + Cz + D = 0 \tag{19}$$

In order for direction (18) to be inclined to plane (19) at angle ϕ, the following condition needs to be satisfied

$$\frac{Aa + Bb + Cc}{\sqrt{(A^2 + B^2 + C^2)}\sqrt{(a^2 + b^2 + c^2)}} = \sin \phi \tag{20}$$

A, B, C and D in equations (19) and (20) are functions of co-ordinates of points A_0, B_1 and A_1, and, thus, functions of the only unknown co-ordinate, z, of point A_1. This co-ordinate is computed from equation (20). Having found z for point A_1, the same procedure is followed for plane $A_1B_1A_2$, where co-ordinate z of point A_2 is now the only unknown, etc.

Analytical geometry relations were also used to compute the volumes and areas of blocks. Each pentahedral block was divided into three tetrahedrons (the only hexahedral block was first divided into two pentahedrons), with the volume of each tetrahedron being

$$\text{volume} = \frac{1}{6}\left|\begin{vmatrix} x_1 & y_1 & z_1 & 1 \\ x_2 & y_2 & z_2 & 1 \\ x_3 & y_3 & z_3 & 1 \\ x_4 & y_4 & z_4 & 1 \end{vmatrix}\right| \tag{21}$$

where x_i, y_i and z_i ($i = 1, 2, 3, 4$) are the co-ordinates of the corner points of the tetrahedrons. The areas of the discontinuity surfaces were computed using the analytical expression for the area of a triangle in 3-D space (quadrangles were first divided into triangles)

$$S = \frac{1}{2}\sqrt{\left[\begin{vmatrix} y_2 - y_1 & z_2 - z_1 \\ y_3 - y_1 & z_3 - z_1 \end{vmatrix}^2 + \begin{vmatrix} z_2 - z_1 & x_2 - x_1 \\ z_3 - z_1 & x_3 - x_1 \end{vmatrix}^2 + \begin{vmatrix} x_2 - x_1 & y_2 - y_1 \\ x_3 - x_1 & y_3 - y_1 \end{vmatrix}^2\right]} \tag{22}$$

where x_i, y_i and z_i ($i = 1, 2, 3$) are the co-ordinates of the triangle's corner points.

REFERENCES

Azzouz, A. S. & Baligh, M. M. (1983). Loaded areas on cohesive slopes. *J. Geotech. Engng. Div. Am. Soc. Civ. Engrs* **109**, 724–729.

Baligh, M. M., Azzouz, A. S. & Ladd, C. C. (1977). Line loads on cohesive slopes. *Proc. 9th Int. Conf. Soil Mech., Tokyo* **2**, 13–17.

Baligh, M. M. & Azzouz, A. S. (1975). End effects on stability of cohesive slopes. *J. Geotech. Engng Div. Am. Soc. Civ. Engrs* **101**, 1105–1117.

Bishop, A. W. (1955). The use of the slip circle in the stability analysis of slopes. *Géotechnique* **5**, No. 1, 7–17.

Bliz, P., Brödel, C. & Reinhardt, K. (1981). Spatial calculation of slope stability under definite surcharges. *Proc. 10th Int. Conf. Soil Mech., Stockholm* **3**, 367–371.

Cavounidis, S. (1987). On the ratio of factors of safety in slope stability analyses. *Géotechnique* **37**, No. 2, 207–210.

Chen, R. H. & Chameau, J. L. (1982). Three-dimensional limit equilibrium analysis of slopes. *Géotechnique* **32**, No. 1, 31–40.

Chen, W. F. (1975). *Limit analysis and soil plasticity.* Amsterdam: Elsevier.

Chen, W. F., Giger, M. W. & Fang, H. Y. (1969). On the limit analysis of stability of slopes. *Soils Fdns* **9**, 23–32.

Chen, W. F. & Giger, M. W. (1971). Limit analysis of stability of slopes. *J. Soil Mech. Fdns Div. Am. Soc. Civ. Engrs* **97**, SM1, 19–26.

Collins, I. F. (1974). A note on the interpretation of Coulomb's analysis of the thrust on a rough retaining wall in terms of the limit theorems of plasticity theory. *Géotechnique* **24**, No. 1, 106–108.

Drescher, A. (1983). Limit plasticity approach to piping in bins. *J. Appl. Mech.*, **50**, 549–553.

Drucker, D. C., Greenberg, H. J. & Prager, W. (1952). Extended limit design theorems for continuous media. *Quart. Appl. Math.* **9**, 381–389.

Fellenius, W. (1927). *Erdstatishe Berechnungen.* Berlin: Ernst.

Gens, A., Hutchinson, J. N. & Cavounidis, S. (1988). Three-dimensional analysis of slides in cohesive soils. *Géotechnique* **38**, No. 1, 1–23.

Hill, R. (1948). A variational principle of maximum plastic work in classical plasticity. *Quart. J. Mech. Appl. Math.* **1**, 18–28.

Hovland, H. J. (1977). Three-dimensional slope stability analysis method. *J. Geotech. Engng Div. Am. Soc. Civ. Engrs* **103**, 971–986.

Janbu, N. (1957). Earth pressures and bearing capacity calculations by generalized procedure of slices. *Proc. 4th Int. Conf. on Soil Mech., London* **2**, 207–212.

Leshchinsky, D., Baker, R. & Silver, M. L. (1985). Three dimensional analysis of slope stability. *Int. J. Numer. Analyt. Meth. Geomech.* **9**, 199–223.

Morgenstern, N. R. & Price, V. E. (1965). The analysis of the stability of general slip surfaces. *Géotechnique* **15**, No. 1, 79–93.

Spencer, E. (1967). A method of analysis of the stability of embankments assuming parallel inter-slice forces. *Géotechnique* **17**, No. 1, 11–26.